



Preparation of high purity cadmium with micro-spherical architecture from zinc flue dust

Yuan LIU, Ya-jie ZHENG, Zhao-ming SUN

School of Metallurgy and Environment, Central South University, Changsha 410083, China

Received 21 July 2014; accepted 5 December 2014

Abstract: This research has focused on the treatment of zinc flue dust by an acid leach process, combining an environmentally suitable impurity removal process to recover cadmium. Optimum conditions were found as follows: H_2SO_4 concentration 90 g/L, liquid/solid ratio 6:1, leaching temperature 60 °C and leaching time 1.0 h. Under these conditions, 95.8% cadmium was recovered. FeAsO_4 and $\text{Fe}(\text{OH})_3$ precipitates with FeCl_3 are found to be highly effective to obtain a high degree of separation of heavy metals and the oxyanions of arsenic from the leachate. The overall separation of arsenic and other heavy metals and precipitate settling rates are optimum at $n(\text{Fe})/n(\text{As})$ ratio of 3:1 and pH 6. The removal rates of Fe, Pb and Cu from the solution were greater than 98.9%, and As removal rate was 99.6%. A solvent extraction with P204 was used for the separation of zinc and cadmium. Optimum conditions are obtained as follows: 20% P204 (volume fraction) diluted with kerosene at room temperature, pH 3.0, and varying organic/aqueous (O/A) phase ratio 1:1. The extraction rate of zinc is 99.2% under these conditions. Spherical cadmium particles showing nearly uniform size were produced by hydrogen reduction at 310 °C and the crystal structure was cubic. In addition, the purity of the recovered cadmium powder is more than 99.99%.

Key words: zinc flue dust; impurity removal; micro-spherical; cadmium powder

1 Introduction

A part of cadmium is recovered from different secondary resources such as zinc ash, zinc dross, flue dust of roasting furnace and brass smelting, nickel–cadmium (Ni–Cd) batteries, which contain different levels of impurities depending on the sources [1]. The chemical nature of these dust particles is classified as hazardous waste. The disposal of such materials is now becoming expensive because of increasingly stringent environmental protection regulations [2–4]. Improved material management can lead to better utilization of refined materials, decreased use of primary materials and energy resources and a reduced need for landfill areas [5,6]. Zinc concentrate is roasted to remove the sulfur from the concentrate and produces impure zinc oxide [7–9]. Inevitably, zinc concentrate contains various contaminants such as cadmium, lead, copper, arsenic and sulfur. Furnace operation generates a hot off-gas containing fume and particulate matter [10]. These resulting gases and fumes are cooled and passed through a bag-house before discharging to atmosphere [11–13].

The roaster dust collected contains base metals, especially lead, cadmium and arsenic [14]. It is thus a toxic product and presents a problem for disposal in an environmentally acceptable way. However, the relatively high cadmium which is present as oxide phase provides a valuable resource. Currently, if the cadmium content of the dust reaches 12% (mass fraction) [15], the dust is mainly returned to the sintering operation for cadmium recovery. Flue dust of zinc smelter, which comes from sintering off-gases in bag-houses [16–18], is a serious problem in terms of pollution and storage because of its high content of hazardous materials such as cadmium, lead, copper, zinc and arsenic and its low apparent density [19,20].

Cadmium has many common industrial uses as it is a key component in battery production [21]. It is present in cadmium pigments and coatings, and is commonly used in electroplating [16,22]. High purity cadmium is widely used in making of II–VI type semiconductors, e.g., HgCdTe [23]. Certain impurities limit the electrical and optical performance in these devices. These may be bulk effects as in the case of γ -ray detectors and modulators or due to the migration of impurities from a

substrate into an epitaxial layer eventually affecting detector performance [24]. High resistivity CdTe crystals with good crystalline quality and a low concentration of defects are needed for room temperature nuclear radiation detectors [25]. Hence, the main limiting factor in the performance of CdTe or CdHgTe is the purity of raw materials [26]. Such impurities at very low levels in high purity cadmium must be developed for the assessment of purity of the starting materials.

This paper describes a laboratory-scale study of a method for producing a high purity cadmium powder based on leaching and precipitation of arsenic in the presence of iron at a pH of 5.5, leaving a residue of metals together with ferric hydroxide. Separation of zinc from the solution is treated by solvent extraction with the acidic extractant di(2-ethylhexyl) phosphoric acid (D2EHPA). Then, the cadmium containing in the solution precipitates with sodium hydroxide. This paper presents an experimental study on the preparation of cadmium powder by reduction of $\text{Cd}(\text{OH})_2$ with hydrogen in a tube furnace. In our experiments, reaction zone temperature is considered the key process variable for the control of particle size and product composition.

2 Experimental

2.1 Materials and analysis methods

The roaster dust was from Yuguang Gold and Lead Group Co., Ltd., Henan, China. The content of impurities was analyzed by inductively coupled plasma optical emission spectroscopy (ICP, IRIS intrepid XSP, Thermo Electron Corporation). The products of cadmium powder were characterized by X-ray diffraction (XRD, Rint-2000, Rigaku). The morphology was measured by scanning electron microscope (JEOL, JEM-5600LV) with an accelerating voltage of 20 kV. Thermal gravimetric analysis (TGA) and differential thermal analysis (DTA) were carried out using Perkin-Elmer TGA and DTA system on well ground samples in flowing nitrogen atmosphere at a heating rate of $5^\circ\text{C}/\text{min}$.

2.2 Experimental procedure

2.2.1 Sulfuric acid leaching

Leaching of the dried powder was carried out in a three-necked glass reactor (500 mL). A thermometer was fitted to one of the openings. The reactor was heated in a mantle to the required temperature and controlled at the desired temperature. The temperature during the leaching experiments could be controlled to be $\pm 2^\circ\text{C}$. The reactor was filled with H_2SO_4 and the sample was added to a preheated acid solution. The stirring speed was kept constant at 400 r/min throughout all the experiments. The

operating variables of acid concentration (30, 70, 90 and 110 g/L), temperature (25, 40, 50, 60 and 70°C) and liquid/solid ratio (4:1, 5:1, 6:1, 7:1 and 8:1) were investigated. At the end of each leaching experiment, the solutions were filtered. The cadmium and other impurities in the solution were determined using an inductively coupled plasma. The leaching residue was dried in an oven at 105°C for 12 h, subjected to X-ray diffraction.

2.2.2 Purification

After the leaching process, the purification experiments were taken for the leaching solution. A typical treatment procedure involved addition of 30% H_2O_2 (mass per volume) to the solution. The mixture was stirred to oxidize the As (III). At this point, FeCl_3 was added and the solution was further stirred. The pH was adjusted with NaOH solution (6 mol/L) and the final step involved filtering off the solid ferric arsenate using nylon membrane filters. The filtered samples were analyzed for the residual arsenic, iron and other impurities concentrations using an inductively coupled plasma (ICP) emission spectrometer.

2.2.3 Solvent extraction

The extractant D2EHPA was used to separate zinc from the solution. The reactive component $(\text{C}_8\text{H}_{17}\text{O})_2\text{PO}_2\text{H}$ is di(2-ethylhexyl)phosphoric acid. The relative molecular mass is 322 and the density at 20°C is $0.974\text{ g}/\text{cm}^3$. The extractant was used without further purification. In all experiments, aviation kerosene was used as organic diluent. All experiments were conducted in a 500 mL three-necked round bottomed reactor in a heating jacket, which was fitted with a stirrer, a thermometer and a pH electrode. The organic phase and aqueous phase were contacted for 10 min by stirring and the pH was controlled by small addition of 4 mol/L H_2SO_4 . The solvent extraction separation was carried out in a separation funnel of 150 mL. After each extraction stage, the mixture was left to stand still for 20 min, permitting the complete separation of the phases. Then, a sample of the solution was withdrawn to measure the zinc and cadmium contents by ICP.

2.2.4 Hydrogen reduction

A tube furnace was used to conduct hydrogen reducing experiments. 10 g $\text{Cd}(\text{OH})_2$ powder was put in a ceramic boat and pushed forward to the reaction zone of the tube furnace. The samples were heated to different temperatures for different durations in a quartz tube. During the heating process, nitrogen gas was introduced to the quartz tube and mixed with hydrogen when the given temperature was reached. Gases were supplied from a gas tank at a flow rate of about 1.0 L/min and room temperature. At the end of each batch reducing, the residues in the boat were collected for XRD analysis.

3 Results and discussion

3.1 Analysis of zinc flue dust

The elemental (Pb, Cd, Zn, Cu, As, K, Na and Fe) analysis results of dust samples are summarized in Table 1. As expected, all dust samples contain Pb, Cd as major elements. The remaining elements to complete to 100% state of the elementary analyses are expected to be S, O, Si and metals at trace levels. All the reagents used for chemical analysis were of analytical grade and of purity greater than 99.9%.

Table 1 Main chemical components of roasting dust (mass fraction, %)

Pb	Cd	Zn	Cu	Fe	As	K	Na
42.45	18.32	0.20	0.09	0.02	0.51	0.99	0.08

XRD pattern (Fig. 1) provides direct evidence of the crystallized compounds in the dusts.

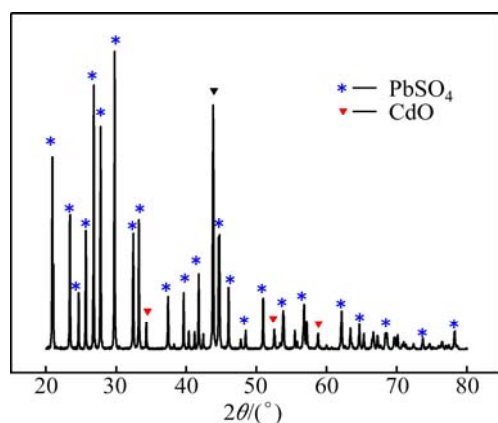


Fig. 1 XRD pattern of zinc flue dust

The major phases in the dusts are found to be PbSO_4 , whereas element cadmium is represented as CdO . Zinc sulfide could not be quantified because of its too small amount.

3.2 Leaching process

3.2.1 Effect of acid concentration

A plot of the leaching rates of Cd and its concomitant metals against acid concentrations was presented in Fig. 2 under the condition that 50 g zinc smelting dust was leached at 60 °C for 1.0 h and liquid/solid ratio 6:1.

The results indicated that the dissolution of Cd and part of its concomitant metals are strongly dependent on the increase in the acid concentration. When acid concentration increased from 30 to 90 g/L, the leaching rate of Cd increased greatly from 65% to 94.1%. The leaching rate dropped at the acid concentration of 130 g/L as the high acid concentration increased the

viscosity of the solution and reduced the diffusion rate of the ions. An initial H_2SO_4 concentration of 90 g/L is necessary to obtain the high leaching rate of Cd.

3.2.2 Effect of liquid/solid ratio

The effect of liquid/solid ratio (from 3:1 to 7:1) on the rate of Cd extraction was investigated with H_2SO_4 concentration of 90 g/L at 60 °C. It can be confirmed from the variation of the leaching rate with various liquid/solid ratios illustrated in Fig. 3 that increasing liquid/solid ratio is beneficial for the leaching of Cd. An increase in the ratio of liquid to solid is expected to reduce the viscosity of reactants for facilitating well mixing and contributing to the reduction of mass transfer resistance in diffusion. Additionally, the variation of the leaching rate is not significant, as the liquid/solid ratio is more than 6:1. Therefore, the liquid/solid ratio of 6:1 is selected as the operational parameter for the leaching process in the consideration of recovery efficiency and reagent dosage.

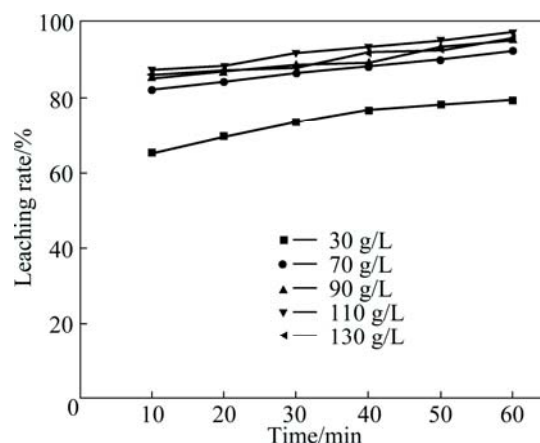


Fig. 2 Effect of acid concentration on leaching rate of Cd

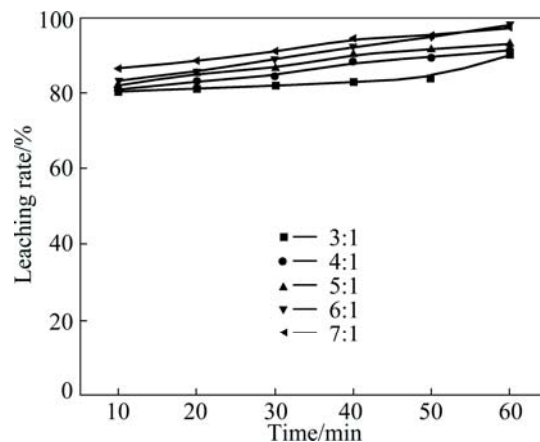


Fig. 3 Effect of liquid/solid ratio on leaching rate of Cd

3.2.3 Effect of leaching temperature

A series of experiments were carried out at 40, 50, 60, 70, 80 °C to investigate the effect of the temperature on leaching rate. The H_2SO_4 concentration and

liquid/solid ratio were kept constant at 90 g/L and 6:1, respectively.

As presented in Fig. 4, the increase in reaction temperature improves the leaching rate at various leaching time. When reaction temperature increases from 40 °C to 60 °C, the leaching rate of roasting products is enhanced from 84.1% to 94.1% in 1.0 h. Additionally, the variation of the leaching rate is not significant, as the temperature is more than 70 °C. The reason for significant improvement on the leaching rate most likely is that the increase of temperature accelerates the molecules thermal motion and increases the contact surface between single particle and leaching agent, and that the barrier of products layer becomes thinner and diffusion flux increases with the temperature rising [21].

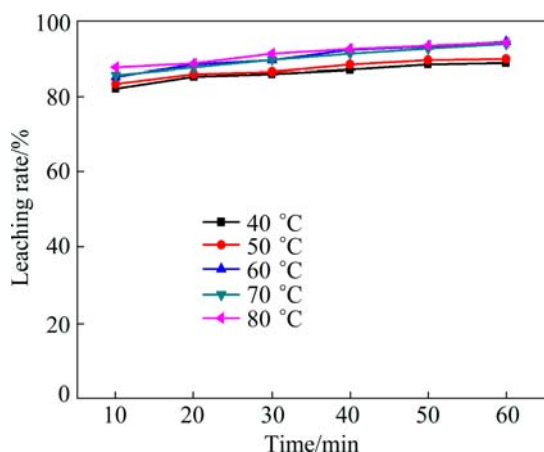


Fig. 4 Effect of leaching temperature on leaching rate of Cd

3.3 Purification

After the leaching process, the purification experiments were taken for the leaching solution which contained about 0.45 g/L As(III), 1.05 g/L As(V), and small amounts of iron (0.07 g/L), copper (0.1 g/L), and zinc (0.2 g/L). Therefore, the formation of As or Fe is also intensified, and thus the purification periods would be necessary for an effective separation following the leaching.

The method involved the oxidation of As (III) with 30% H₂O₂:



followed by the addition of FeCl₃ at Fe/As mole ratios of 1.0–4.0 and neutralization to precipitate FeAsO₄ according to the reaction:



3.3.1 Effect of pH

The effect of pH (from 1 to 8) on the impurities removal rate was investigated with stirring speed of 400 r/min at room temperature.

When the pH was changed from 1 to 6, Fe and Cu

reached its high removal rate at 99.3% and 96.7%, respectively, while most of the arsenic precipitated as ferric arsenate.

Increasing the pH may improve the removal rate of arsenic, but it will also increase the cadmium consumption (Fig. 5). This trend, the decreasing arsenic removal rate in the solution with the pH=8, may be interpreted as a reflection of the equilibrium of ferric arsenate with AsO₄³⁻ via Reaction (3) [27]. Therefore, pH 6 was selected as the optimum pH for impurity remove process.

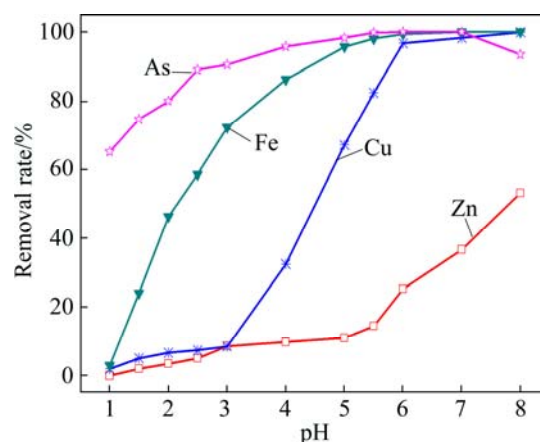


Fig. 5 Effect of pH on removal rate of impurities

3.3.2 Effect of Fe/As mole ratio

The next set of experiments was carried out to determine the minimum total iron dose required for optimal impurity removal at pH 6. A constant range of Fe/As mole ratio, between 1.0:1 and 4.0:1, was used, while the amount of 30% H₂O₂ used is 10 times of theoretical dosage. The results from these experiments were used to formulate the Fe/As mole ratio profile presented in Fig. 6.

The arsenic precipitation rate increased with

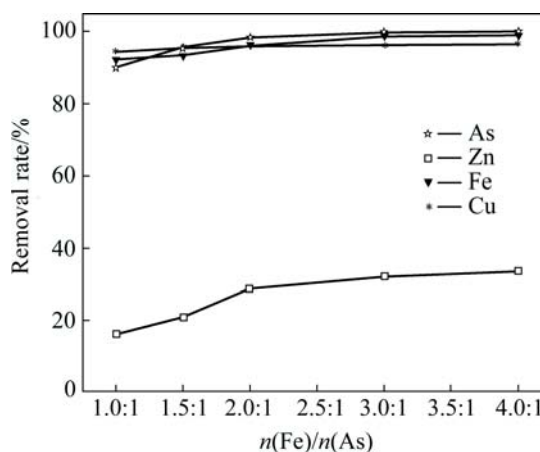


Fig. 6 Effect of Fe/As mole ratio on removal rate of impurities

increasing Fe/As mole ratio in the initial solution. The Fe/As mole ratio affected the arsenic precipitation rate in a similar but less marked way when the Fe/As mole ratio reached 2.0:1. Arsenic concentrations dropped to below the detection limits at a total Fe/As mole ratio of 3.0:1 which is observed for the optimal arsenate removal experiment.

3.4 Solvent extraction

According to SILVA et al [28], the selectivity of P204 for zinc extraction lies in the pH range of 2.0–4.5. Single-stage extraction from the liquor was carried out with 20% (volume ratio) P204 diluted with kerosene under the conditions of room temperature, pH 3.0, and varying organic / aqueous (O/A) phase ratios (Fig. 7).

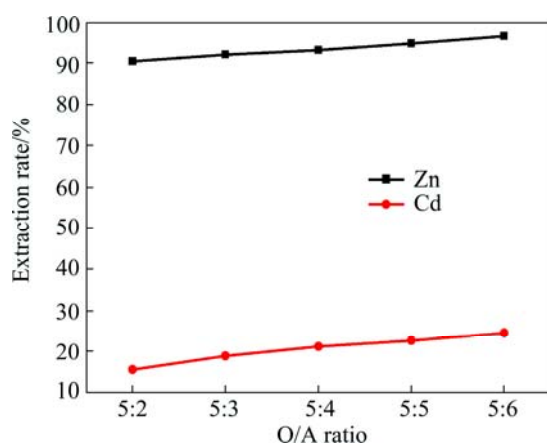


Fig. 7 Effect of O/A ratio on zinc extraction

At a phase ratio of 1:1, about 99% zinc was extracted from the aqueous phase, but about 23% of cadmium was co-extracted. The extraction tests at pH 3.0 and five different P204 concentrations were carried out according to the results shown in Fig. 8, in which the extraction rates were observed for ions in the leaching solution. The extraction rate is found to increase with increasing P204 concentration in volume fraction.

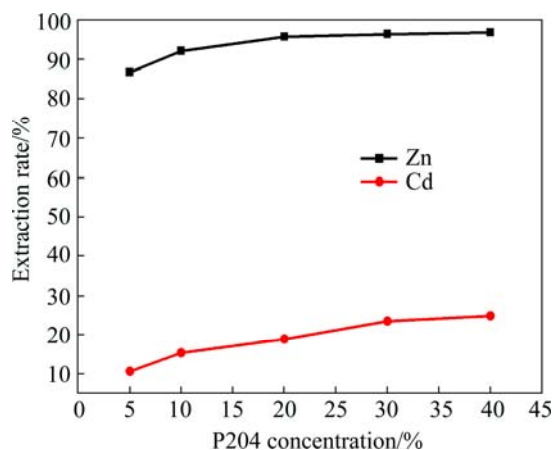


Fig. 8 Effect of P204 concentration on zinc extraction

3.5 Precipitation and hydrogen reduction

After the selective zinc extraction, cadmium was precipitated at room temperature and pH 9.0 with addition of NaOH solution (6 mol/L). $\text{Cd}(\text{OH})_2$ obtained was separated from the solution, washed with ultra pure water and alcohol. Residual cadmium ion content in the solution was less than 0.5 mg/L. Impurity contents of $\text{Cd}(\text{OH})_2$ are shown in Table 2.

Table 2 Impurity contents of $\text{Cd}(\text{OH})_2$ (mg/kg)

Zn	Pb	Cu	Ag	As	Fe
0.6	0.2	0.1	0.3	0.3	0.3

For the micro-structural analysis, the as-synthesized sample was directly transferred to SEM chamber without disturbing the original nature of the product. Figure 9 shows the morphology of $\text{Cd}(\text{OH})_2$ prepared with 6 mol/L NaOH precipitated at room temperature.

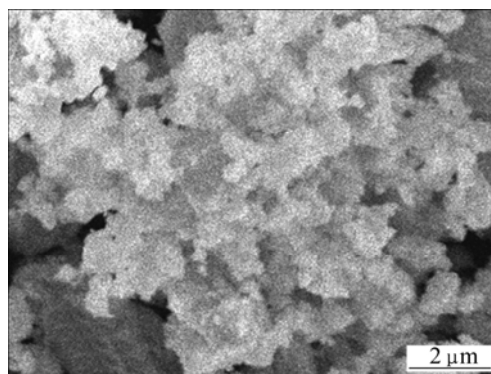


Fig. 9 SEM image of $\text{Cd}(\text{OH})_2$ powder

The TG–DTA curves for the sample are shown in Fig. 10.

$\text{Cd}(\text{OH})_2$ is decomposed to CdO and H_2O according to the following reaction:

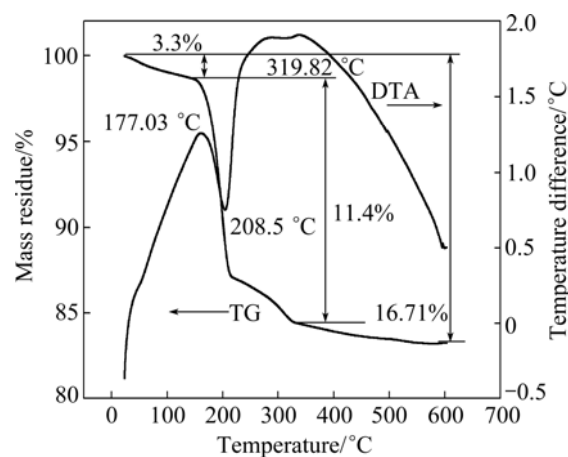
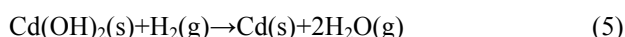


Fig. 10 TG/DTA curves of $\text{Cd}(\text{OH})_2$ powder

Two distinct mass losses are observed. The initial mass loss of about 3.3 % observed in TG curve at 130 °C is due to the evaporation of physically adsorbed water. The other is ascribed to the conversion of hydroxide to oxide. The subsequent major mass loss of ~11.4% found with the DTA curve endothermic peak near 208.5 °C is related to the decomposition of Cd(OH)₂ into CdO and H₂O. The TG result is well within the theoretical mass loss.

The reaction of Cd(OH)₂ and H₂ can be described as follows:



XRD pattern was used to investigate the changes of phase structure of the products at different temperatures. Figure 11 shows the XRD patterns of the Cd(OH)₂ powder reduced by hydrogen at various temperatures. At 250 °C and 280 °C, the diffraction peaks of both CdO and Cd phases were present in the reduced samples. It can be seen that all the diffraction peaks of the samples reduced at 310–340 °C could be indexed with the phase of Cd. With increasing reduction temperature from 280 to 310 °C, the peak intensities of CdO decreased significantly, indicating that the phase transformation temperature was 280 °C. When the reduction temperature reached 310 °C, only Cd phase was found in the XRD pattern, indicating a narrow temperature range of phase transformation.

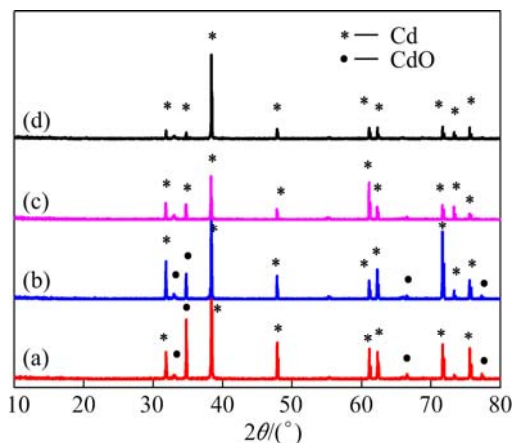


Fig. 11 XRD patterns of Cd(OH)₂ powder reduced at different temperatures: (a) 250 °C; (b) 280 °C; (c) 310 °C; (d) 340 °C

Figure 12 shows SEM micrographs of the products. The spherical morphology was obviously observed. The temperature of reactants was found to be an effective factor for particle size. As the temperature increased, the average particle size became larger and size distribution became more non-uniform. At 310 °C, cadmium powders ranging from 10 to 50 μm in average particle sizes were produced. The impurity contents of the product are shown in Table 3.

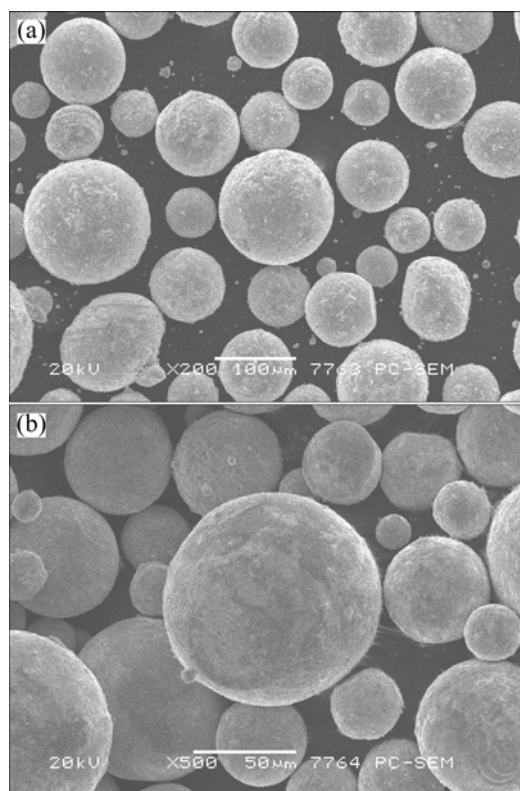


Fig. 12 SEM images of Cd powders reduced at 310 °C (a) and 340 °C (b)

Table 3 Impurity contents of Cd powder (mg/kg)

Zn	Pb	Cu	Ag	As	Fe
0.1	0.2	0.1	0.1	0.2	0.1

As stated above, the cadmium from zinc flue dust could be recovered with purity higher than 99.99%. Especially, the recovered Cd powder had a wide range of application such as nuclear radiation detector and solar cells.

4 Conclusions

1) Sulfuric acid was used as a leachant and 96% cadmium was dissolved under the optimum conditions: 60 °C, 90 g/L H₂SO₄, liquid/solid (volume ratio) 6:1, and leaching time of 1.0 h. The leach residue was present as PbSO₄.

2) The optimum conditions for arsenic removal conducted on the acid leaching solution were found to be: Fe/As mole ratio of 3.0:1, pH 6, stirring at 400 r/min for 30 min. A solvent extraction with P204 was used for the separation of zinc and cadmium.

3) As the reaction zone temperature increased, the particle diameter and the conversion of Cd(OH)₂ increased. Throughout present experiments, spherical cadmium particles showing nearly uniform size were

produced at 310 °C and the crystal structure was cubic. The purity of the recovered cadmium powder was higher than 99.99%.

References

- [1] ZHU Jian-xin, LI Jin-hui, NIE Yong-feng, YU Bo. Recovery of cadmium by high-temperature vacuum evaporation from Ni–Cd batteries [J]. Transactions of Nonferrous Metals Society of China, 2003, 13(2): 254–257.
- [2] HU Bao-yun, JING Zhen-zi, HUANG Jian-feng, YUN Jun. Synthesis of hierarchical hollow spherical CdS nanostructures by microwave hydrothermal process [J]. Transactions of Nonferrous Metals Society of China, 2012, 22(S1): s89–s94.
- [3] ZHANG Jin, WANG Bo-xiong, YE Li-na. Design and development of portable intelligent testing and charging equipment for nickel-cadmium battery [J]. Journal of Electronic Measurement and Instrument, 2010, 24(4): 359–364.
- [4] EROL M, KUCUKBAYRAK S, ERSOY-MERICBOYU A. The influence of the binder on the properties of sintered glass–ceramics produced from industrial wastes [J]. Ceramics International, 2009, 35(7): 2609–2617.
- [5] IKHMAYIES S J, AHMAD-BITAR R N. AC measurements of spray-deposited CdS: In thin films [J]. Journal of Central South University, 2012, 19(3): 829–834.
- [6] EVIS Z, YILMAZ B, USTA M, AKTUG S L. X-ray investigation of sintered cadmium doped hydroxyapatites [J]. Ceramics International, 2013, 39(3): 2359–2363.
- [7] RABBANI M M, NAM D G, KIM D H, WEONTAE O H. Characterization of Au/CdTe nanocomposites prepared by electrostatic interaction [J]. Transactions of Nonferrous Metals Society of China, 2013, 23(2): 426–432.
- [8] SAFARZADEH M S, BAFGHI M S, MORADKHANI D, IIKHCHI M O. A review on hydrometallurgical extraction and recovery of cadmium from various resources [J]. Minerals Engineering, 2007, 20(3): 211–220.
- [9] YANG Bo, WANG Cheng-yan, LI Dun-fang, YIN Fei, CHEN Yong-qiang, WANG Nian-wei. Selective separation of copper and cadmium from zinc solutions by low current density electrolysis [J]. Transactions of Nonferrous Metals Society of China, 2010, 20(3): 533–536.
- [10] ULMANU M, MARANON E, FERNANDEZ Y, CCASTRILLON L, ANGER I, DUMITRIUN D. Removal of copper and cadmium ions from diluted aqueous solutions by low cost and waste material adsorbents [J]. Water, Air, and Soil Pollution, 2003, 142(1–4): 357–373.
- [11] SAFARZADEH M S, MORADKHANI D, IIKHCHI M O. Determination of the optimum conditions for the cementation of cadmium with zinc powder in sulfate medium [J]. Chemical Engineering and Processing: Process Intensification, 2007, 46(12): 1332–1340.
- [12] XU Zhi-feng, LI Qiang, NIE Hua-ping. Pressure leaching technique of smelter dust with high-copper and high-arsenic [J]. Transactions of Nonferrous Metals Society of China, 2010, 20(S1): s176–s181.
- [13] CUI Ji-rang, ZHANG Li-feng. Metallurgical recovery of metals from electronic waste: A review [J]. Journal of Hazardous Materials, 2008, 158(2–3): 228–256.
- [14] FAN Xing-xiang, YANG Bo. Research on the technologies for separating valuable elements from the fly ash bearing Zn, Ni and Cd and preparing relative products [J]. Multipurpose Utilization of Mineral Resources, 2009, 4: 14–16.
- [15] ROSENQVIST T. Principles of extractive metallurgy [M]. Trondheim, Norway: Tapir Academic Press, 2004.
- [16] BOPARAI H K, JOSEPH M, CARROLL D M. Kinetics and thermodynamics of cadmium ion removal by adsorption onto nano zerovalent iron particles [J]. Journal of Hazardous Materials, 2011, 186: 458–465.
- [17] DU Xin-ling, ZHANG Xin, MA Ke-you. Industrialized production of pure cadmium [J]. China Nonferrous Metallurgy, 2010(4): 25–28. (in Chinese)
- [18] DHIVYA P, PRASAD A K, SRIDHARAN M. Nanostructured cadmium oxide thin films for hydrogen sensor [J]. International Journal of Hydrogen Energy, 2012, 37(23): 18575–18578.
- [19] HIRSCH H, LIANG S, WHITE A. Preparation of high-purity cadmium, mercury, and tellurium [J]. Semiconductors and Semimetals, 1981, 18: 21–45.
- [20] HUANG Kui, LI Jia, XU Zhen-ming. Characterization and recycling of cadmium from waste nickel–cadmium batteries [J]. Waste Management, 2010, 30(11): 2292–2298.
- [21] WU Xuan, YU Yi-fu, LIU Yang, LIU Cui-bo, ZHANG Bin. Synthesis of hollow Cd₂Zn_{1-x}Se nanoframes through the selective cation exchange of inorganic–organic hybrid ZnSe–amine nanoflakes with cadmium ions [J]. Angewandte Chemie, 2012, 124(13): 3265–3269.
- [22] VISWANATH S G, SAJIMOL G. Electrowinning of nickel powder from glycerol and ammonical medium–study of morphology and nano-nature of the powder [J]. Metallurgical and Materials Engineering, 2012, 18(2): 129–143.
- [23] ROGALSKI A. HgCdTe infrared detector material: History, status and outlook [J]. Reports on Progress Physics, 2005, 68(10): 2267–2336.
- [24] ALBIN D S, DEMTSU S H, MCMAHON T J. Film thickness and chemical processing effects on the stability of cadmium telluride solar cells [J]. Thin Solid Films, 2006, 515(4): 2659–2668.
- [25] CHATTOPADHYAY K, FETH S, CHEN H, BURGER A, SU C H. Characterization of semi-insulating CdTe crystals grown by horizontal seeded physical vapor transport [J]. Journal of Crystal Growth, 1998, 191(3): 377–385.
- [26] KRISHNA M V, SHEKHAR R, KARUNASAGAR D, ARUNACHALAM J. Multi-element characterization of high purity cadmium using inductively coupled plasma quadrupole mass spectrometry and glow-discharge quadrupole mass spectrometry [J]. Analytica Chimica Acta, 2000, 408 (1–2): 199–207.
- [27] LE BERRE J F, GAUVIN R. Demopoulos, characterization of poorly-crystalline ferric arsenate precipitated from equimolar Fe(III)–As(V) solutions in the pH range 2 to 8 [J]. Metallurgical and Materials Transactions B, 2007, 38(5): 751–762.
- [28] SILVA J E, PAIVA A P, SOARES D, LABRINCHA A, CASTRO F. Solvent extraction applied to the recovery of heavy metals from galvanic sludge [J]. Journal of Hazardous Materials, 2005, 120(1–3): 113–118.

以锌冶炼烟尘为原料制备高纯微球形貌镉粉

刘 远, 郑雅杰, 孙召明

中南大学 冶金与环境学院, 长沙 410083

摘 要: 采用酸浸和对环境友好的除杂方法处理锌冶炼烟尘回收提取高纯镉。结果表明, 其最佳条件如下: 硫酸浓度 90 g/L、液固比 6:1、反应温度 60 °C、浸出时间 1.0 h, 此条件下镉的浸出率达 95.8%。采用 FeCl₃ 沉淀生成 FeAsO₄ 和 Fe(OH)₃ 来分离重金属和砷, 当 $n(\text{Fe})/n(\text{As})$ 为 3:1、pH=6.0 时, 铁、铅和铜的去除率均超过 98.9%, 砷的去除率为 99.6%。P204 用于锌和镉的溶剂萃取分离, 最佳萃取条件如下: P204 浓度 20%(体积分数, 室温下用煤油稀释)、pH=3、相比 O/A=1:1。在此条件下, 锌的萃取率为 99.2%。当还原温度为 310 °C 时, 镉粉的形貌为均匀球形, 晶体结构为立方晶体, 得到的镉粉纯度超过 99.99%。

关键词: 锌烟尘; 除杂; 微球; 镉粉

(Edited by Wei-ping CHEN)